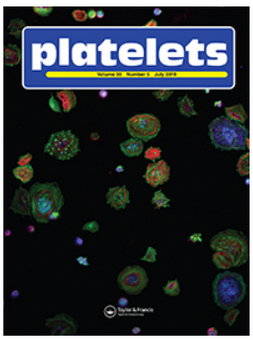

Platelets

ISSN: 0953-7104 (Print) 1369-1635 (Online) Journal homepage: https://www.tandfonline.com/loi/iplt20

Morphological and optical properties of human immature platelet-enriched population produced in immunodeficient mice

Mari Kono, Shiori Matsuhiroya, Fumie Nakazawa, Masako Kaido, Atsushi Wada & Yoshiaki Tomiyama

To cite this article: Mari Kono, Shiori Matsuhiroya, Fumie Nakazawa, Masako Kaido, Atsushi Wada & Yoshiaki Tomiyama (2019) Morphological and optical properties of human immature platelet-enriched population produced in immunodeficient mice, Platelets, 30:5, 652-657, DOI: 10.1080/09537104.2018.1501013

To link to this article: https://doi.org/10.1080/09537104.2018.1501013

Published online: 30 Jul 2018.

http://www.tandfonline.com/iplt
ISSN: 0953-7104 (print), 1369-1635 (electronic)

Platelets, 2019; 30(5): 652–657

DOI: https://doi.org/10.1080/09537104.2018.1501013

ORIGINAL ARTICLE

Morphological and optical properties of human immature platelet-enriched population produced in immunodeficient mice

Mari Kono[1], Shiori Matsuhiroya[1], Fumie Nakazawa[1], Masako Kaido[1], Atsushi Wada[1], & Yoshiaki Tomiyama[2]

[1]*Scientific Affairs, Sysmex Corporation, Nishi-ku, Kobe, Japan and* [2]*Department of Blood Transfusion, Osaka University Hospital, Suita, Osaka, Japan*

Abstract

Ultrastructure analysis of immature platelets is difficult because of the lack of a suitable marker and their relatively low concentration in total platelets.

We investigated the morphological and optical properties of human immature platelets produced and enriched in immunodeficient mice via human CD34-positive cell administration. Immunodeficient mice were injected with human CD34-positive cells and administered eltrombopag orally for 14 days (eltro-mice). Some of these mice were maintained for 2–3 months (steady-state-mice). Platelets were double-stained with a human CD41 antibody and a nuclear staining dye (Sysmex hematology analyzer XN series reagent), and then analyzed by flowcytometry FCM to identify human immature platelets. Human CD41-positive cells were isolated from citrated blood by magnetic cell sorting with human CD41 antibody, and examined using electron microscopy.

Flow cytometric analysis with the XN reagent demonstrated that peripheral blood from eltro-mice had a higher percentage of immature platelet fraction in human platelets than that from steady-state-mice. The geometric mean of XN reagent fluorescence for human platelets, divided with that for mouse platelets, revealed that the ratios in eltro-mice were significantly higher than those in steady-state-mice, thus indicating that immature platelets were highly enriched in eltro-mice. Scanning and transmission electron microscopy revealed that human citrated platelets isolated from eltro-mice tended to be larger (n = 15, p = 0.276) and contained more mitochondria than those isolated from steady-state-mice (n = 10, p = 0.0002).

Therefore, an increased number of mitochondria, rather than platelet size, is a distinctive feature of immature platelets.

Keywords

Electron microscopy, flow cytometry, immature platelets, immunodeficient mice, thrombopoietin

History

Received 21 February 2018
Revised 18 June 2018
Accepted 4 July 2018
Published online 27 July 2018

Introduction

Platelets are enucleated cells which are derived from megakaryocytes in the bone marrow and are present in the blood at concentrations ranging from 150,000 to 400,000 cells/μL (1). When blood vessels are damaged, platelets immediately adhere to the damaged endothelial cells to form a platelet plug and stop bleeding. Owing to their highly polyploid nuclei, megakaryocytes in the bone marrow are large cells (~ 60 μm), with one megakaryocyte releasing approximately 1000 platelets, which are derived from its proplatelets and pass through holes in the bone marrow blood vessels, into the peripheral blood (2). Reticulated platelets (RP) are reported to be young platelets (i.e. immature platelets) that have been recently released into the circulation and are probably analogous to reticulocytes, reflecting erythropoiesis (3). RP can be distinguished from mature platelets by their RNA content, by using flow cytometry (FCM) with an RNA-binding fluorochrome, such as thiazole orange (4,5). In addition, the Sysmex hematology analyzer (XN-series) and Abbott CELL-DYN Sapphire can measure RP as an immature platelet fraction (3). In a Sysmex hematology analyzer, platelets are exposed to a reagent which contains a detergent and fluorescent nuclear staining dye. A two-dimensional scattergram is then plotted, based on the forward scattering light (FSC) intensity (vertical axis) and side fluorescent light (SFL) intensity (horizontal axis), using the principles of FCM. Platelets that display higher intensity of both FSC and SFL are identified as being in the immature platelet fraction (IPF) (6,7). Percentage of IPF (IPF%) values correlate well with RP% values obtained by thiazole orange staining (8). It has been demonstrated that IPF% values, especially when measured using the XN series, as well as RP% values, are useful to determine platelet turnover in thrombocytopenic disorders, and for predicting platelet recovery after stem cell transplantation (8–14).

Immature platelets (and RP) have been reported to be larger than mature platelets (4,15). However, the morphological properties of immature platelets are difficult to observe, owing to the lack of suitable markers and their presence at a relatively low percentage in total platelets. Most previous studies have reported observations of immature platelets derived from megakaryocytes

Color versions of one or more of the figures in the article can be found online at www.tandfonline.com/iplt.

Correspondence: Mari Kono, Scientific Affairs, Sysmex Corporation, 1-3-2 Murotani, Nishi-ku, Kobe 651-2241, Japan. E-Mail: Kono.Mari@sysmex.co.jp

in vitro, but these results cannot accurately represent the morphology of immature platelets *in vivo*, as they do not take into account the effects of shear stress that platelets are subjected to in the body (16).

In this study, we produced and enriched human immature platelets in the body of NOD/Shi-scid, IL-2Rγ KO Jic (NOG) mice injected with human CD34-positive cells, by concomitant oral administration of eltrombopag for 14 days. Eltrombopag stimulates the production of human pluripotent stem cells and megakaryocytes, but not murine cells (17). The ultrastructural analysis of human immature platelets isolated using anti-human CD41 antibody revealed that immature platelets tended to be larger and contained higher number of mitochondria.

Methods

Animals

Eight-week-old NOD/Shi-scid, IL-2Rγ KO Jic (NOG) mice (Central Institute for Experimental Animals, Kanagawa, Japan) were maintained in sterilized cages under a 12-h light/dark cycle. The animals were fed a pellet chow and sterilized tap water *ad libitum*. Human CD34-positive cells (1×10^5) from cord blood (AllCells, CA, USA) were transplanted through the tail vein after irradiation with 2.5 Gy. Eltrombopag at 25 mg/kg body weight (Revolade, GlaxoSmithKline, Middlesex, UK) was orally administrated every day for 14 days (17). As shown in Figure 1, after 14-day administration of eltrombopag, mice were designated as eltro-mice. Some of the mice were maintained for 2–3 months after the 14-day administration, and these mice were designated as steady-state-mice. Mice that were transplanted with human CD34-positive cells without eltrombopag were designated as control-mice (Figure 1).

Blood

Citrated or EDTA-anticoagulated peripheral blood was collected from the hearts of all the mice. Platelet-rich-plasma (PRP) samples were prepared from the citrated peripheral blood samples by centrifugation at $160 \times g$ for 20 min. EDTA blood samples were analyzed using an XN-2000 (Sysmex, Kobe, Japan) and a platelet analysis scattergram (PLT-F scattergram), to obtain the value of IPF%.

FCM analysis

EDTA-anticoagulated peripheral blood samples were incubated with FITC-conjugated anti-human CD41 (Platelet Glycoprotein llb) mouse monoclonal antibody (Clone 5B12, F7088, DAKO, Glostrup, Denmark) solution, at a concentration of 15 μ mol/L in phosphate-buffered saline (PBS) for 30 min at 4°C. FITC-conjugated mouse IgG1 antibody (DAKO) was used as a negative control. Blood samples stained with the antibody were then exposed to specific reagents: CELLPACK DFL and Fluorocell PLT of the XN series (Sysmex). Five microliters of the sample, 1000 μL of DFL, and 20 μL of Fluorocell PLT, were gentry mixed in a manner similar to that in case of XN, and were excited by a 642-nm laser and detected by a 660-nm filter laser using a FCM (EC800 Cell Analyzer, Sony Corporation, Tokyo, Japan), approximately after 2 minutes-incubation at room temperature.

Magnetic cell sorting

The PRP samples were fixed with 1.5% paraformaldehyde in PBS and stained with biotin-conjugated human CD41 mouse monoclonal antibody (Clone P2, IM0718, Beckman Coulter, CA, USA) at a concentration of 2 mg/L in PBS for 30 min at 4°C. Human CD41-positive platelets were then isolated from the PRPs by biotin-positive selection using the magnetic cell sorting system (STEMCELL Technologies, British Columbia, Canada) as per the manufacturer's instructions.

Scanning electron microscopy

Isolated human CD41-positive platelets were fixed in 1% glutaraldehyde (Electron Microscopy Sciences, Hatfield, PA) in PBS for 16 h at 4°C. The fixed cells were then attached to poly-L-lysine-coated glass slides. After fixation and dehydration using the same method as that used for transmission electron microscopy (TEM), the ethanol was replaced with t-butyl alcohol (Wako Pure Chemicals, Osaka, Japan). These samples were then dried using a freeze-dryer (Hitachi High-Technologies) and decorated with osmium using Neoc (MEIWAFOSIS, Tokyo, Japan). JSM-7500F (Nippon-Denshi, Osaka, Japan) was used for scanning electron microscopy (SEM) analysis. Images of discoid

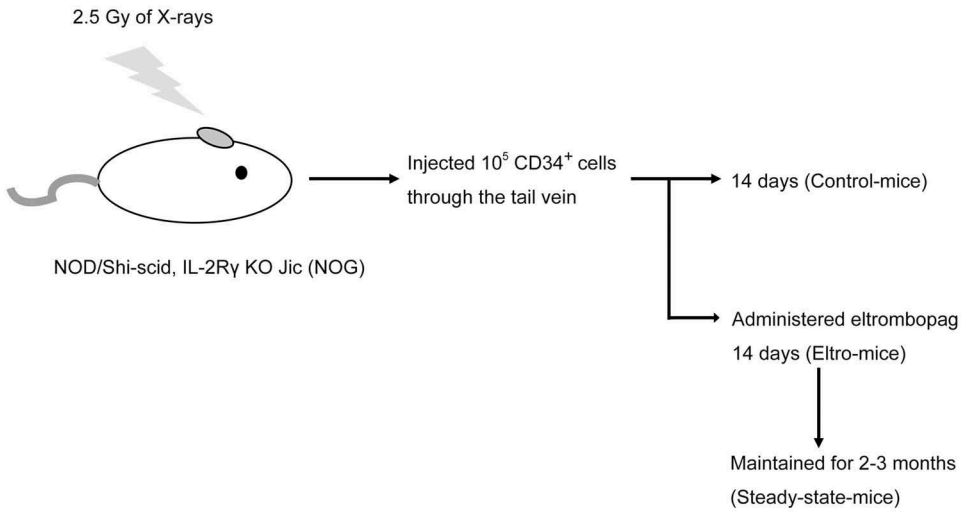

Figure 1. Procedure using immunodeficiency mice.
Mice after 14 day-administration of eltrombopag were designated as eltro-mice. Mice maintained for 2–3 months after the 14-day administration were designated as steady-state-mice. Mice that were transplanted with human CD34-positive cells without eltrombopag, were designated as control-mice.

shape platelets were used for measuring the area using ImageJ 1.49V (National Institutes of Health, Maryland, USA). 15 images obtained from 3 different eltro-mice and 17 images obtained from 4 different steady-state-mice were analyzed by two operators independently.

Transmission electron microscopy

For transmission electron microscopy (TEM) analysis, isolated human CD41-positive platelets were fixed in 1% glutaraldehyde (Electron Microscopy Sciences) in PBS for 16 h at 4°C. The fixed cells were then attached to silanized glass slides using Cytospin® (Thermo Fisher Scientific, Massachusetts, USA) and post-fixed in 1% osmium tetroxide for 45 min at 4°C. Following osmium fixation, the samples were dehydrated in a graded series of ethanol and invert-embedded in Quetol 812 (Nisshin EM, Tokyo, Japan). The samples were then cut into 80–100 nm sections using an Ultracut UCT ultramicrotome (Leica Microsystems, Wetzlar, Germany) and imaged using an H-7500 transmission electron microscope (Hitachi High-Technologies, Tokyo, Japan). We analyzed 10 images obtained from 3 different eltro-mice and 11 images obtained from 4 different steady-state-mice. The number of all the mitochondria in stable platelets that could be recognized by the human eye was counted from the TEM images by two operators independently.

Statistical analysis

Normal distribution of data was confirmed using the Kolmogorov-Smirnov test and F test, performed using EZR version 1.32 (Jichi medical University, Tokyo, Japan). Welch's t-test was employed to compare the two groups.

Results

Analysis for IPF% in eltro-mice and steady-state-mice

The intensity of peripheral blood samples double-stained with a FITC-conjugated human CD41 antibody (Figures 2(a) and 2(c) right) or the negative control antibody (Figures 2(a) and 2(c) left), along with the XN series reagent specific for nucleic acids, was measured using FCM.

FITC intensity along the vertical axis (Figures 2(a) and 2(c)) indicated that the ratio percentage of human CD41-positive cells events in the total platelets was 4.95% in eltro-mice, and 17.28% in steady-state-mice (Figures 2(a) and 2(c), red dots). To examine IPF % in these mice, human and mouse platelets were stained with XN reagent as shown in Figures 2(b) and 2(d). Estimated IPF% values were 18.39% and 6.08% for human platelets in eltro-mice and steady-state mice, respectively. Geometric means of each red color fluorescent intensity for human platelets were 331.01 and 295.64, in eltro-mice and steady-state mice, respectively. We calculated the ratios of human geometric mean to mouse geometric mean, as the total platelet number was markedly different between

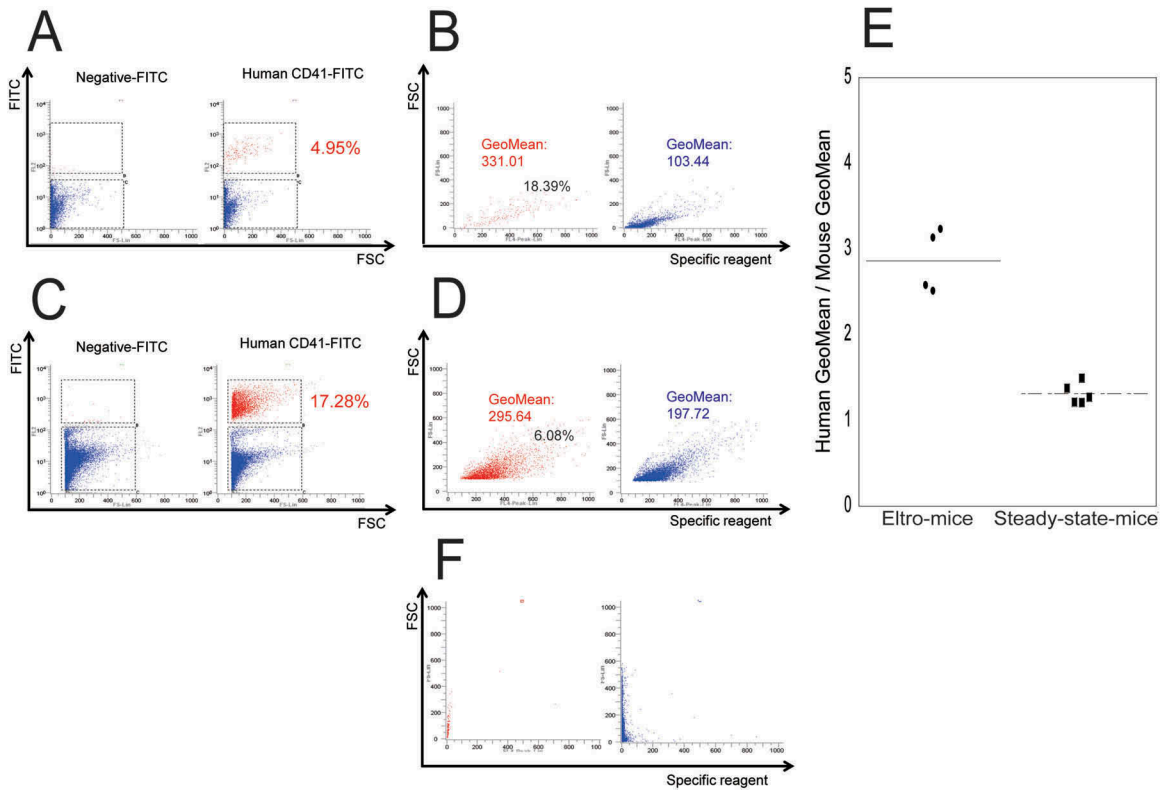

Figure 2. FCM analysis of peripheral blood samples obtained from eltro-mice and steady-state-mice.
Peripheral blood was obtained from eltro-mice (A and B) or steady-state-mice (C and D). The blood samples were double-stained with FITC-conjugated human CD41 (right of panels) or negative (left of A and C) antibody as well as a Sysmex exclusive reagent of the XN series. FSC intensity is shown on the horizontal axis and FITC intensity is shown on the vertical axis (A and C). FITC-positive (red) and -negative (blue) platelets were gated in the right panels of A and C, and represented in B or D. The intensity of the Sysmex exclusive reagent is shown on the horizontal axis and FSC intensity is shown on the vertical axis (B and D). For the analysis of positive particles in B and D, we set the gate where no positive particles were detected without the Sysmex exclusive reagent (F).The numbers in red in A and C represent human platelets as a percentage of the total number of observed platelets. The numbers indicated in B and D represent the geometric mean of specific reagent intensities of red or blue dots, and representative data are shown ($n \geq 4$). IPF% of human platelets were estimated (black letters in left of panels B and D). The geometric mean of specific reagent intensity for human platelets/geometric mean for mouse platelet ratios are described as the dotplots. The average are shown as lines ($n \geq 4$) (E). $^{**}p < 0.01$.

eltro-mice and steady-state-mice. The ratio was approximately 1 in steady-state mice, while it increased by approximately three-times in eltro-mice ($p < 0.01$, Figure 2(e)). eltro-mice human thrombopoiesis, but not mice thrombopoiesis, could be stimulated by eltrombopag administration. Thus, these data strongly suggested that as compared with steady-state-mice, IPF% values for human platelets were markedly increased in eltro-mice.

In addition, we analyzed peripheral blood samples in eltro-mice using an XN-2000. In the XN analysis, both human and mouse platelets were examined, as the XN did not distinguish human platelets from mouse platelets. IPF% values were significantly higher than those obtained from control-mice which had not received eltrombopag ($2.05 \pm 0.37\%$ vs. $0.38 \pm 0.05\%$, $n \geqq 4$, $p < 0.01$).

Taken together, both data strongly suggested that in eltro-mice, immature platelets are significantly enriched in the peripheral blood, as compared with those in steady-state-mice or control-mice. Thus, we further examined the morphological characteristics of immature platelets enriched in peripheral blood obtained from eltro-mice.

Morphological analysis by electron microscopy

To confirm that we examined human platelets, and not mouse platelets, magnetic bead (white arrows)-positive platelets, without activation, were observed using SEM (Figure 4). For the morphological analysis we used citrated blood samples. Before the analysis, we preliminarily examined IPF% in citrated samples. Estimated IPF% value was 33.33%, which was much higher than that in EDTA-samples (33.33% in citrated samples vs 18.39% in EDTA samples)(data not shown). The difference was probably because platelet morphology is more properly maintained in citrated blood. To compare platelet size between eltro-mice and steady-state-mice, human platelets were randomly selected, and the area of each was calculated from the SEM images. Immature platelet-enriched samples obtained from eltro-mice appeared larger than those from steady-state-mice, although the difference was not statistically significant ($n = 15$, $p = 0.276$).

We also examined enriched immature platelets by TEM. TEM samples from the same mice ($n = 3$) as those used for SEM analysis. Figure 5 shows the surface connecting systems (SCS), granules (G), and mitochondria with inner membrane (yellow arrows), in magnetic bead (white circles)-positive platelets. We calculated the number of mitochondria in each platelet and found that the number was significantly higher in human platelets obtained from eltro-mice than from steady-state-mice ($n = 10$, $p = 0.0002$).

Discussion

IPF% (and RP%) values are useful biomarkers to distinguish platelet consumptive disorder, such as primary immune thrombocytopenia (ITP), from hypoplastic thrombocytopenia, such as aplastic anemia (AA). They are also useful for predicting thrombopoietic recovery after stem cell transplantation and/or chemotherapy (8,9,18,19).

However, the morphological characteristics of immature platelets have not been well documented. In this study, we investigated the morphological and optical properties of human immature platelets *ex vivo*, which were produced in immunodeficient mice by the injection of human CD34-positive cells, with concomitant stimulation with a human-specific thrombopoietin receptor agonist (eltrombopag). The immunodeficient NOD/Shi-scid, IL-2Rγ KO Jic (NOG) mice lack T cells, B cells, NK cells, and the IL-2 receptor, and possess low activity macrophages (20). When CD34-positive cells are injected into these mice, stable human platelets are produced in the body of the mice three months later (21–23). To stimulate human thrombopoiesis, but not mouse thrombopoiesis, we orally administered eltrombopag, a thrombopoietin receptor agonist, which has been used in patients with aplastic anemia as well as in patients with primary immune thrombocytopenia (17). Histidine residue 499, located in the transmembrane domain of the thrombopoietin receptor, *c-Mpl*, is human-specific, and is essential for the effects of eltrombopag (17).

We first examined whether oral administration of eltrombopag for 14 days might increase IPF% for human platelets in peripheral blood obtained from eltro-mice, compared with that from steady-state-mice. In eltro-mice the proportion of human platelets was only 4.95%, while in steady-state-mice it was 17.28%. We also confirmed that after 14 days post-bone marrow transplantation of human hematopoietic stem cells into control mice without eltrombopag, human platelets were hardly produced in the mice (data not shown). The proportion of immature platelets was significantly higher in eltro-mice than in steady-state-mice, probably due to the stimulation of human thrombopoiesis by eltrombopag administration (Figs. 2 and 3). However, IPF% on Figure 3 was lower than Figure 2, because XN did not distinguish human platelets from mouse platelets. To evaluate human immature platelets more precisely in eltro-mice, we used the mouse geometric mean for the XN reagent as a control. As shown in Figure 2(e), the ratio of the human geometric mean to the mouse geometric mean was markedly increased in eltro-mice. These data confirmed that IPF% was markedly increased in eltro-mice, compared with steady-state-mice.

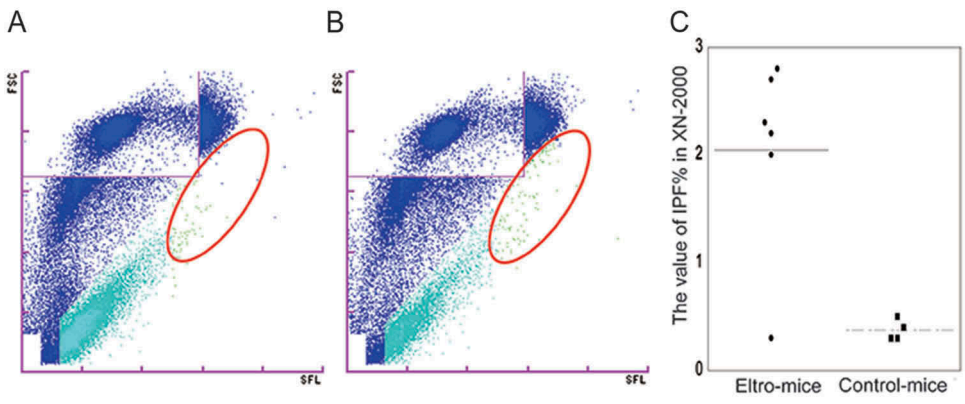

Figure 3. XN analysis of the peripheral blood samples.
Peripheral blood samples were obtained from eltro-mice or control-mice, and were analyzed using the XN series. Representative PLT-F scattergram from the XN-series is shown (A and B). Red circles indicate IPF area. The values of IPF% are shown as the dotplots. The average are shown as lines (n = 4–6) (C). $^{**}p < 0.01$.

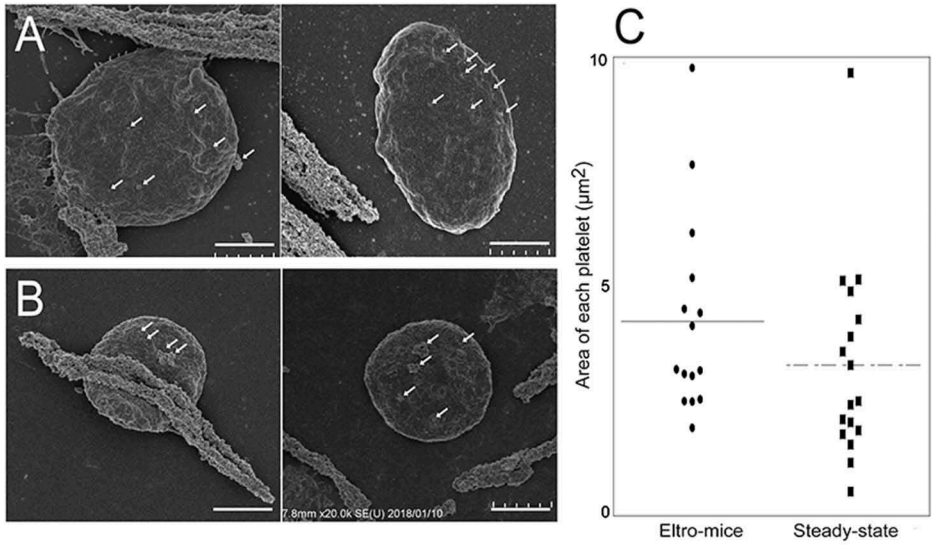

Figure 4. SEM observation of human CD41-positive platelets.
Human CD41-positive cells were isolated from the PRP from eltro-mice (A) or steady-state-mice (B). Representative magnetic bead-attached human CD41-positive platelets are shown. The values of areas from the SEM images are shown as the dotplots. The average are shown as lines (n = 15–17) (C). Scale Bar = 1 μm. White arrows in A and B indicate magnetic beads.

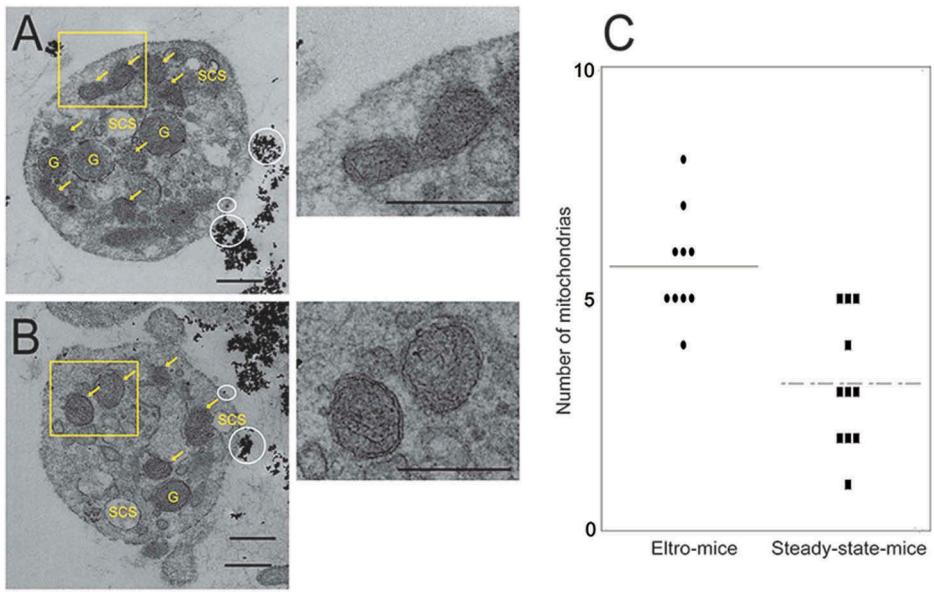

Figure 5. TEM observation of human CD41-positive platelets.
Human CD41-positive cells were isolated from the PRP from eltro-mice (A) or steady-state-mice (B). Representative magnetic bead-attached human CD41-positive platelets are shown. The numbers of mitochondria in each platelet observed with TEM are shown as the dotplots. The average are shown as lines (n = 10–11) (C). Scale Bar = 1 μm. White circles in A and B indicate magnetic beads. Yellow arrows indicate mitochondria. G: granules, SCS: surface connecting systems. Right panels of A and B are high magnification images of yellow rectangles. ***$p < 0.001$.

We then performed a morphological analysis of human platelets obtained from eltro-mice and steady-state-mice. Human platelets were isolated by magnetic beads coated with anti-human CD41. We only examined magnetic bead-positive platelets by electron microscopy to confirm that the platelets examined were of human origin. Our ultrastructural analysis suggested that immature platelets might be larger that mature platelets, which is consistent with previously published data (4,15). However, our data did not show a statistically significant difference in platelet size between eltro-mice and steady-state-mice. This is probably because we examined immature platelet-enriched blood samples, and not isolated immature platelet samples. Nonetheless, our data clearly demonstrated that immature platelet-enriched samples from eltro-mice contained significantly higher numbers of mitochondria than those from steady-state-mice. These data revealed that the most distinctive feature of immature platelets may be an increased number of mitochondria, rather than the large size of platelets. For the morphological analysis, we used citrated blood samples. Before the analysis, we preliminarily examined IPF% in citrated samples. The estimated IPF% value was 33.33%, which is much higher than that in EDTA-samples (33.33% in citrated samples vs 18.39% in EDTA samples on Figure 2(b)) (data not shown). The difference was probably because platelet morphology is more properly maintained in citrated blood.

Recently, we characterized platelet organelles, stained using the XN reagent, and revealed that XN reagent staining

overlapped with anti-Grp75 staining, a mitochondrial marker protein (7). Thus, the XN reagent mainly stains mitochondria (probably mitochondrial DNA and RNA) and cytosolic mRNA in platelets. These data are consistent with the data presented in this study that immature platelets contain increased numbers of mitochondria.

In summary, we enriched human immature platelets by employing a unique experimental model in which human CD34-positive cells were transplanted into immunodeficient mice with concomitant stimulation of a human-specific thrombopoietin receptor agonist (eltrombopag). The protocol of this study had the certain limitations, because which immature human platelets could not be completely isolated. However, this ultrastructural analysis demonstrated that the number of mitochondria is a more useful marker for immature platelets than the platelet size. Our present data further contributes to our understanding of the characteristics of immature platelets.

Declaration of interest

YT reports consultant fees from Sysmex.

Funding

This work was supported by the Ministry of Education, Culture, Sports, Science and Technology in Japan [Grant-in Aid for Scientific Research]; Ministry of Health, Labor and Welfare in Japan [Grant-in Aid for Scientific Research]; This study was funded by Sysmex Corporation.

References

1. Partric JS. Chapter 154 Platelets. In: Walker HK, Hall WD, Hurst JW, editors. Clinical Methods: the history, physical, and laboratory examinations. 3rd edition. Boston: Butterworths;1990;728–731
2. Junt T, Schulze H, Chen Z, Massberg S, Goerge T, Krueger A, Wagner, D D., Graf, T., Italiano, J E., Shivdasani, R A., et al. Dynamic visualization of thrombopoiesis within bone marrow. Science 2007;317:1767–1770. doi:10.1126/science.1146304
3. Dusse LM, Freitas LG. Clinical applicability of reticulated platelets. Clin Chim Acta 2015;439:143–147. doi:10.1016/j.cca.2014.10.024
4. Ingram M, Coopersmith A. Reticulated platelets following acute blood loss. Br J Haematol 1969;17:225–229. doi:10.1111/j.1365-2141.1969.tb01366.x
5. Dale GL. Platelet kinetics. Curr Opin Hematol 1997;4:330–334. doi:10.1097/00062752-199704050-00006
6. Hamaguchi Y, Kondo T, Nakai R, Ochi Y, Okazaki T, Uchihashi K, Morikawa T. Overview of the automated hematology analyzer XN-serirs. Sysmex Journal International 2015; 25: 1–12.
7. Wada A, Takagi Y, Kono M, Morikawa, T., Colombo, G I. Accuracy of a New Platelet Count System (PLT-F) depends on the staining property of its reagents. PLoS One 2015;10:e0141311. doi:10.1371/journal.pone.0141311
8. Sakuragi M, Hayashi S, Maruyama M, Kiyokawa, T., Nagamine, K., Fujita, J., Maeda, T., Kato, H., Kashiwagi, H., Kanakura, Y., et al. Immature platelet fraction (IPF) as a predictive value for thrombopoietic recovery after allogeneic stem cell transplantation. Int J Hematol 2018;107:320–326. doi:10.1007/s12185-017-2344-8
9. Sakuragi M, Hayashi S, Maruyama M, Kabutomori, O., Kiyokawa, T., Nagamine, K., Kato, H., Kashiwagi, H., Kanakura, Y., Tomiyama, Y. Clinical significance of IPF% or RP% measurement in distinguishing primary immature thrombocytopenia from aplastic thrombocytopenic disorders. Int J Hematol 2015;101:369–375. doi:10.1007/s12185-015-1741-0
10. Briggs C, Kunka S, Hart D, Oguni, S., Machin, S J. Assessment of an immature platelet fraction (IPF) in peripheral thrombocytopenia. Br J Haematol 2004;126:93–99. doi:10.1111/j.1365-2141.2004.04987.x
11. van der Linden N, Klinkenberg LJ, Meex SJ, Beckers, Erik A.M., De Wit, Norbert C.J., Prinzen, L. Immature platelet fraction measured on the Sysmex XN hemocytometer predicts thrombopoietic recovery after autologous stem cell transplantation. Eur J Haematol 2014;93:150–156. doi:10.1111/ejh.12319
12. Parco S, Vascotto F. Application of reticulated platelets to transfusion management during autologous stem cell transplantation. Onco Targets Ther 2012;5:1–5. doi:10.2147/OTT.S27883
13. Park SH, Park CJ, Kim MJ, Han, M.-Y., Lee, B.-R., Cho, Y.-U., Jang, S., Kwon, S.-W., Kim, D.-Y., Lee, J.-H., et al. Evaluation of parameters obtained from the Sysmex XN-2000 for predicting the recovery of the absolute neutrophil count and platelets after hematopoietic stem cell transplantation. Int J Lab Hematol 2016; Feb 2. 2016; doi:10.1111/ijlh.12470
14. Barsam SJ, Psaila B, Forestier M, Page, L K., Sloane, P A., Geyer, J T., Villarica, G O., Ruisi, M M., Gernsheimer, T B., Beer, J H., et al. Platelet production and platelet destruction: assessing mechanisms of treatment effect in immune thrombocytopenia. Blood 2011;117:5723–5732. doi:10.1182/blood-2010-11-321398
15. Karpatkin S. Human platelet senescence. Annu Rev Med 1972;23:101–128. doi:10.1146/annurev.me.23.020172.000533
16. Falcieri E, Bassini A, Pierpaoli S, Luchetti, F., Zamai, L., Vitale, M., Guidotti, L., Zauli, G. Ultrastructural characterization of maturation, platelet release, and senescence of human cultured megakaryocytes. Anat Rec 2000;258:90–99. doi:10.1002/(ISSN)1097-0185
17. Kuter DJ. The biology of thrombopoietin and thrombopoietin receptor agonists. Int J Hematol 2013;98:10–23. doi:10.1007/s12185-013-1382-0
18. Kurata Y, Hayashi S, Kiyooi T, Kosugi, S., Kashiwagi, H., Honda, S., Tomiyama, Y. Diagnostic value of tests for reticulated platelets, plasma glycocalicin, and thrombopoietin levels for discriminating between hyperdestructive and hypoplastic thrombocytopenia. Am J Clin Pathol 2001;115:656–664. doi:10.1309/RAW2-0LQW-8YTX-941V
19. Kuwana M, Kurata Y, Fujimura K, Tonnu, L. Preliminary laboratory based diagnostic criteria for immune thrombocytopenic purpura: evaluation by multicenter prospective study. J Thromb Haemost 2006;4:1936–1943. doi:10.1111/j.1538-7836.2006.02117.x
20. Ito M, Hiramatsu H, Kobayashi K, Layton, D M., Mawby, W J., Stewart, G W., Oldenborg, P-A., Delaunay, J., Tanner, Michael J A. NOD/SCID/gamma(c)(null) mouse: an excellent recipient mouse model for engraftment of human cells. Blood 2002;100:3175–3182. doi:10.1182/blood-2001-12-0207
21. Garcia S, Freitas AA. Humanized mice: current states and perspectives. Immunol Lett 2012;146:1–7. doi:10.1016/j.imlet.2012.03.009
22. Goyama S, Wunderlich M, Mulloy JC, Spina, D., Cleary, S J., Wakelam, M J., Page, C P., Pitchford, S C., Welch, Heidi C E. Xenograft models for normal and malignant stem cells. Blood 2015;125:2630–2640. doi:10.1182/blood-2014-11-570218
23. Yamane A, Nakamura T, Suzuki H, Szabolcs, P., Driscoll, T A., Page, K., Lakshminarayanan, S., Allison, J., Wood, S., Semmel, D., et al. Interferon-alpha 2b-induced thrombocytopenia is caused by inhibition of platelet production but not proliferation and endomitosis in human megakaryocytes. Blood 2008;112:542–550. doi:10.1182/blood-2007-12-125906